Regional differences in Chinese SO_2 emission control efficiency and policy implications

Qianqian Zhang[1,2], Yuxuan Wang[1,3,4], Qiao Ma[1,2], Yu Yao[1], Yuanyu Xie[1], Kebin He[2]
[1]Ministry of Education Key Laboratory for Earth System Modeling, Center for Earth System Science, Institute for Global Change Studies, Tsinghua University, Beijing, China
[2]School of Environment, Tsinghua University, Beijing, 100084, China
[3]Department of Marine Sciences, Texas A&M University at Galveston, Galveston, TX, 77553, USA.
[4]Department of Atmospheric Sciences, Texas A&M University, College Station, TX, 77843, USA.

Correspondence to: Yuxuan Wang (yxw@tsinghua.edu.cn)

Abstract

SO_2 emission control has been one of the most important air pollution policies in China since 2000. In this study, we assess regional differences in SO_2 emission control efficiencies in China through the modeling analysis of four scenarios of SO_2 emissions, all of which aim at reducing the national total SO_2 emissions by 8% or 2.3 Tg below the 2010 emissions level, the target set by the current 12th Five-Year Plan (FYP) (2011-2015), but differ in the spatial implementation. The GEOS-Chem chemical transport model is used to evaluate the efficiency of each scenario on the basis of four impact metrics: surface SO_2 and sulfate concentrations, population-weighted sulfate concentration (PWC), and sulfur export flux from China to the Western Pacific. The efficiency of SO_2 control (β) is defined as the relative change of each impact metric to a 1% reduction of SO_2 emissions from the 2010

baseline. The S1 scenario, which adopts a spatially uniform reduction of SO_2 emissions in China, gives a β of 0.99, 0.71, 0.83, and 0.67 for SO_2 and sulfate concentrations, PWC, and export flux, respectively. By comparison, the S2 scenario, which implements all the SO_2 emissions reduction over North China (NC), is found most effective in reducing national-mean surface SO_2 and sulfate concentrations and sulfur export fluxes, with β being 1.0, 0.76 and 0.95 respectively. The S3 scenario of implementing all the SO_2 emission reduction over South China (SC) has the highest β in reducing PWC ($\beta = 0.98$) because SC has the highest correlation between population density and sulfate concentration. Reducing SO_2 emissions over Southwest China (SWC) is found to be least efficient on the national scale, albeit big within-region benefits. The difference in β by scenario is attributable to the regional difference in SO_2 oxidation pathways and source-receptor relationship. Among the three regions examined here, NC shows the largest proportion of sulfate formation through gas phase oxidation, which is more sensitive to SO_2 emission change than aqueous oxidation. In addition, NC makes the largest contribution to inter-regional transport of sulfur within China and to the transport fluxes to Western Pacific. The policy implication is that China needs to carefully design a regionally specific implementation plan of realizing its SO_2 emissions reduction target in order to maximize the resulting air quality benefits not only for China but for the downwind regions, with emphasis on reducing emissions from NC where SO_2 emissions have decreased at a slower rate than national total emissions in the previous FYP period.

1. Introduction

SO_2 is the precursor of ambient sulfate, which is a major component of particulate matter with dynamic diameter less than 2.5 μm ($PM_{2.5}$) and makes up about 20-35% of total $PM_{2.5}$ mass (Pathak et al., 2009). SO_2 emissions from China contribute about 25% of global SO_2 emissions and 50% of Asian emissions (Streets et al., 2003; Lu et al., 2011). Since 2000, the Chinese government has made great efforts in controlling SO_2 emissions in order to reduce atmospheric PM concentrations and acid deposition. A 10% SO_2 emission reduction target was set in both the tenth Five-Year Plan (10^{th} FYP, 2000-2005) and the 11^{th} FYP (2006-2010). While SO_2 emissions increased about 28% during the 10^{th} FYP (Schreifels et al., 2012), by the end of the 11^{th} FYP China has achieved the goal of 10% SO_2 emission reduction in 2010 relative to the 2005 level (Lu et al., 2011). Itahashi et al. (2012a) reported that aerosol optical depths (AOD) retrieved from the Moderate Resolution Imaging Spectroradiometer (MODIS) over East Asia showed an increase from 2001 to 2005 and then a decrease until 2010, consistent with the reported trend of SO_2 emissions from China.

In 2012, $PM_{2.5}$ was introduced into China's ambient air quality standard by the Ministry of Environmental Protection (MEP). In response to the increasingly severe haze pollution, the Action Plan on Prevention and Control of Air Pollution was delivered by the Central Government of China in September 2013. Aiming to improve air quality across China in the next five to ten years, the Action Plan calls for more efforts to reduce emissions from the heavily polluted regions in East China (22 °-42 °N, 110 °-122 °E). The Action Plan requires that by 2017, $PM_{2.5}$ concentrations should

decrease by 25% over the Beijing-Tianjin-Hebei region, 20% over the Yangtze River Delta, and 15% over the Pearl River Delta. While the Action Plan presents guidelines and advice for energy consumption and cleaner production, like other laws and regulations in China there is no specific emission control target for primary PM or its gaseous precursors for the whole country or by specific regions.

The purpose of this study is to assess the regional differences in SO_2 emission control efficiency in China and discuss the implications for future emission control strategies. We choose four impact metrics to evaluate the efficiency of different scenarios of SO_2 emissions reduction. The first two metrics are surface concentrations of SO_2 and sulfate. The GEOS-Chem chemical transport model is used to quantify the response of SO_2 and sulfate concentrations to changes in SO_2 emissions. Since public health is an important issue of concern for $PM_{2.5}$, the third metric is population-weighted sulfate concentration at the surface. SO_2 emissions from China also have significant impacts on air quality and public health of foreign regions due to long-range transport. Park et al. (2004) suggested that trans-Pacific transport of sulfate accounts for 30% of sulfate background in the U.S. Itahashi et al. (2012b) reported that central eastern China is the dominant source region for sulfate aerosols over Oki Island during two air pollution events in July 2005. Previous studies have recognized the Western Pacific as the predominant transport pathway of air pollution exported from China (Heald et al., 2006; Fairlie et al., 2010; Li et al., 2010a; He et al., 2012). Given the global impact of changing Chinese emissions, it is important to understand the response of pollution outflow to different emission control strategies in China.

Therefore, the fourth metric is the outflow flux of sulfur from China to the Western Pacific.

Within the context of currently available emission control plans in China, we design four different spatial realizations of reducing China's total SO_2 emissions by 8% or 2.3 Tg below the 2010 emissions level, which is the target set by the current 12th FYP (2011-2015). In the first scenario SO_2 emissions are reduced uniformly by 8% over China, while in the other three scenarios the emissions reduction is implemented over three different regions which make the largest contributions to the national SO_2 emissions and have highest sulfate concentrations: North China (NC, 33°-42°N, 110°-122°E), South China (SC, 22°-33°N, 110°-122°E), and Southwest China (SWC, 23°-33°N, 102°-110°E) (Figure 1). Since sulfate aerosols exhibit regionally specific formation and transport characteristics (Wang Y et al., 2013a), the response of a given impact metric to the same amount of SO_2 emission reduction is expected to differ by region.

It is clear that the target of 8% reduction of Chinese SO_2 emissions is far from sufficient to meet the goal of reducing $PM_{2.5}$ concentrations set by the Action Plan (Wang Y et al., 2013a). However, there is no other specific target of SO_2 emissions available in current Chinese policies to serve as an alternative reference point. Since our study focuses on the regional difference in emission control efficiency, we choose an 8% perturbation of total SO_2 emissions that is large enough to capture the regional difference.

The paper is organized as follows. Section 2 describes the model and the

evaluation of model results by observations. In Section 3 we present the different reduction scenarios of SO_2 emissions in China and analyze the regionally different responses of the selected impact metrics to those scenarios. Section 4 analyzes sulfate formation and sulfur transport by region to understand the mechanisms behind the regional difference of SO_2 emission control efficiency, followed by sensitivity tests of our results. The concluding remarks are presented in Section 5.

2. Model description and evaluation

2.1 Model description

We use the GEOS-Chem chemical transport model version 9-01-01 to simulate the coupled aerosol-oxidant chemistry on the global and regional scale. The model is driven by the assimilated meteorological data from the Goddard Earth Observation System (GEOS) with 6-hour averaged winds, temperature, cloud and convective mass flux, and 3-hour averaged surface quantities and mixing depths. Here we use the nested-grid capability of GEOS-Chem with a $0.5° \times 0.667°$ horizontal resolution over East Asia, which was originally described by Wang Y (2004) and Chen et al. (2009). The global simulation with a horizontal resolution of $4° \times 5°$ is used to provide boundary conditions for the nested-grid domain.

The sulfate-nitrate-ammonium (SNA) aerosol simulation coupled to the HO_X–NO_X–VOC-ozone gas chemistry was originally developed by Park et al. (2004). Emitted SO_2 in the model is oxidized to sulfate by hydroxyl radicals (OH) in the gas phase and by hydrogen peroxide (H_2O_2) and ozone (O_3) in the aqueous phase. The

gas-particles equilibrium of aerosols is calculated using the ISOROPIA II (Fontoukis and Nenes, 2007) aerosol equilibrium model. The aerosols are removed through dry and wet deposition.

The Global Emission Inventory Activity (GEIA) inventory (Benkovitz et al., 1996) is used in the global simulation, which is overwritten by the NEI05 inventory over the US, the EMEP inventory over Europe, and the INTEX-B inventory over East Asia (Wang Y et al., 2013a). For the nested-grid simulation, the Multi-resolution Emission Inventory for China (MEIC) for the year 2010 is adopted over China (He, 2012) and emissions over the rest of East Asia are taken from the INTEX-B emission inventory. The MEIC inventory uses an improved technology-based methodology to estimate anthropogenic emissions from China, including emissions of SO_2, NO_X, NH_3, BC, OC, NMVOCs, CO, CO_2, and fine and coarse mode PM. The MEIC inventory has an open access dataset for the period from 1990 to 2010 (http://www.meicmodel.org), providing monthly emission data in the horizontal resolution of 0.25°×0.25°, 0.5°×0.5° and 1°×1°. The MEIC emission inventory has been shown to provide good estimation of total emissions with some uncertainties in the spatial allocations for the fine grid resolutions within cities (Wang L. et al., 2014). According to the MEIC inventory, SO_2 emissions from China are 28.4 Tg in 2010 (Figure 1).

2.2 Model evaluation

The GEOS-Chem simulation of sulfate and $PM_{2.5}$ over China has been evaluated by Wang Y et al. (2013a; 2014) and Lou et al. (2014). Wang Y et al. (2013a) indicated

that the GEOS-Chem model had a good performance in simulating sulfate distributions (R^2 = 0.64 ~ 0.79) and concentrations (mean bias of -10%) in East Asia. Lou et al. (2014) reported a higher correlation between simulated and observed sulfate (R^2 = 0.86), but a larger model bias (-41%) which may be partly due to the fact that they used a uniform factor of 0.6 to infer sulfate concentrations in $PM_{2.5}$ from those in observed PM_{10} concentrations. Wang Y et al. (2014) further evaluated the model performance in reproducing the concentrations and the spatiotemporal patterns of $PM_{2.5}$ over China during a severely polluted month of January 2013. The model shows a good correlation of 0.6 with $PM_{2.5}$ spatial distributions but underestimates the concentrations of $PM_{2.5}$ and sulfate over North China during a severe haze period, which is largely explained by underestimated emissions from this heavily polluted region. The sulfate underestimation is further attributed to the heterogeneous reaction of SO_2 on pre-existing aerosols that are deliquescent under the condition of higher relative humidity during the severe haze period (Wang Y et al., 2014). In this study we extend the previous model evaluation by using four additional datasets over China: (1) AOD retrieved from MODIS for January, July, and annual mean of 2010; (2) SO_2 total columns retrieved by the Ozone Monitoring Instrument (OMI) satellite instrument; (3) sulfate concentrations observed at three surface sites in China: the Miyun site (40°29′N, 116°47′N) in NC, the Jinsha site (29°38′N, 114°12′N) in SC (Zhang et al., 2014), and the Chengdu site (30°39′N, 104°2′N) in SWC (Tao et al., 2014); (4) monthly wet deposition fluxes at 5 sites from January 2009 to December 2010, which are from the Acid Deposition Monitoring Network in East Asia (EANET,

181 http://www.eanet.asia/). Locations of all the surface sites used in this study are
182 displayed in Figure 2a.

183 The spatial distributions of AOD over China for annual mean, January and July
184 of 2010 from MODIS (top) and the model (bottom) are displayed in Figure 3. The
185 model shows a strong spatial correlation ($R > 0.6$) with MODIS AOD. Both the model
186 and MODIS indicate higher annual mean AOD in North and South China and a shift
187 of the highest AOD values from central China in January to NC in July. The model
188 has a positive bias of more than 10% for the annual, January, and July mean AOD
189 levels over China as a whole. There is an obvious positive bias of the model over
190 North China, with an overestimation of 26% and 20%, respectively, for the annual and
191 January mean. The model shows a higher correlation (0.73) and smaller bias (12%)
192 over North China in July. The model bias over South China and Southwest China is
193 comparatively smaller and negative at -3% for SC and -1% for SWC. The positive
194 bias of AOD in North China is due to the overestimates of nitrate concentrations
195 (Wang Y et al., 2013a) and overestimation of dust emissions from the
196 Taklimakan-Gobi area which are transported to this region (Wang et al., 2012).

197 Figure 4 compares annual-mean total SO_2 column densities from OMI and
198 GEOS-Chem for 2010. Compared to AOD, satellite-derived SO_2 columns provide a
199 more direct evaluation of sulfur simulation in the model since SO_2 is the direct
200 precursor of sulfate. The original horizontal resolution of the Level 3 OMI data is
201 $0.25° \times 0.25°$, and the GEOS-Chem simulation has a resolution of $0.5° \times 0.667°$. We
202 regridded both OMI and modeled SO_2 columns to $1° \times 1°$ resolution for comparison.

The spatial distribution of SO_2 column densities from GEOS-Chem correlates well with those from OMI, with the correlation coefficient being 0.79, 0.73 and 0.64 for NC, SC and SWC, respectively. Compared with the OMI SO_2 retrievals, GEOS-Chem simulated SO_2 columns are 6% higher in NC, 2% higher in SC and 8% lower in SWC. The discrepancy between the modeled and OMI SO_2 is within ±10% for all the three regions, indicating an overall good simulation of SO_2 by the GEOS-Chem model. Wang Y et al. (2014) reported a 50% underestimate of SO_2 emissions from North China by the GEOS-Chem model for an extremely polluted month of January 2013. Since we used a different bottom-up inventory with higher SO_2 emission from NC and simulated a different year, we did not find evidence that SO_2 emissions were underestimated in winter 2010.

The simulated and observed surface sulfate concentrations at the three surface sites are compared in Figure 5. Weekly-mean sulfate concentrations from January to June 2010 are shown for the Miyun site (Figure 5a). The model agrees well with the observed variability with a correlation of 0.75, and it shows a small positive bias of 4%. Wang Y et al. (2013a) reported a correlation of 0.7 and overestimation of 15% of the model in comparison with the Miyun observations in 2007, using an old version of model and a different anthropogenic emission inventory for China. Similar to Wang Y et al. (2013a), we find here that the model cannot capture the sawtooth-like variation of sulfate during late spring and summer at the Miyun site, which is caused by the model's weakness in simulating large precipitation and high wind speeds at the local scale (Zhang L. et al., 2012). Observations at the Jinsha and Chengdu site are

collected from published literature. Jinsha is a regional background site located in SC (Zhang et al., 2014) and the sampling period was from March 2012 to March 2013. Chengdu is an urban site (Tao et al., 2014) located in SWC and sulfate concentrations were collected during January, April, July and October in 2011. The model has an annual mean bias of 5% at the Jinsha site (Figure 5b) and -8% at the Chengdu site (Figure 5c), with higher seasonal biases partly due to the fact that the simulation and measurements are for different years.

Figure 2b displays the scatter plot of simulated versus observed monthly-mean sulfate wet deposition fluxes from January 2009 to December 2010 at 5 EANET sites in China (Figure 2a). The model reproduces the annual-mean sulfate wet deposition fluxes with a high correlation of 0.83 and small negative bias of -9%. Seasonally, the model tends to overestimate sulfate wet deposition fluxes in the winter (bias = 30%; R = 0.63), but underestimate them in other seasons (R = 0.8 ~ 0.88, biases =-10% ~ -19%).

In summary, through comparison of the model results with satellite-derived AOD and SO_2 columns, surface sulfate observations at three surface sites located in each region, and sulfate wet deposition fluxes for 5 sites in China, we conclude that the model has some capability to reproduce the spatial and temporal distributions of sulfate over China with a small to moderate bias. While the model performance of sulfate and SO_2 simulation differs by site and season, the annual-mean model biases are all within ±10% for the three regions of interest and thus not expected to affect the comparison of the emission scenarios.

3. Efficiency of SO_2 emission control strategies

3.1 Simulation scenarios

In this study, one standard simulation using the 2010 MEIC inventory of Chinese emissions and four sensitivity simulations with different SO_2 emission reduction scenarios (S1 – S4) are conducted, which are described in Table 1. The standard simulation is carried out for the period from January 2009 to December 2010, with the first year for spin up and the next year for analysis. SO_2 emissions from China in 2010 are 28.4 Tg in the standard simulation. All the emission scenarios have an 8% (2.3 Tg) reduction in national total SO_2 emissions below their 2010 level, following the goal of the 12^{th} FYP, but they differ in the spatial distributions of those reductions. In the S1 scenario, the 8% emission reduction is implemented uniformly over the whole country; in the S2, S3, and S4 scenario, the 2.3 Tg reduction of SO_2 emissions is implemented by decreasing regional emissions from three sub-regions of China which make the largest contributions to the national total emissions and have highest sulfate concentrations (Zhang X. Y. et al., 2012; Wang Y et al., 2013a). The three regions are North China (NC, S2 scenario), South China (SC, S3) and Southwest China (SWC, S4). The region definitions are shown in Figure 1. Since the baseline emissions from the three regions are different, the percentage of the emission reduction differs by region, being 21.3%, 29.5% and 48.9% of the baseline emissions from NC, SC and SWC, respectively. A 3-month initialization is conducted for each of the emission reduction scenarios.

Following Lamsal et al. (2011) and Zhang et al. (2014), we define a relationship

between the change of an impact metric (X) and the change of SO_2 emissions (E): $\frac{\Delta X}{X} = \beta \times \frac{\Delta E}{E}$, where ΔX is the change in the metric, with X being surface SO_2 or sulfate concentrations, population-weighted sulfate concentration, or sulfur outflow fluxes from China to Western Pacific,; $\frac{\Delta X}{X}$ is the relative change of the metric; ΔE is the change of SO_2 emissions; $\frac{\Delta E}{E}$ is the relative emission change, which is 0.08 for all the emission reduction scenarios on the national scale; and β is a unitless term describing the relative changes of the metrics of concern in response to a 1% change in SO_2 emissions. We call β the efficiency factor, and it is used to compare the sensitivity of each metric to SO_2 emission changes between different emission reduction scenarios. The larger β, the larger impact SO_2 emission change will have on the related metrics. β tends to be ≤ 1 because the relative rate of change in sulfate will not exceed that of SO_2 emissions. Considering that the emission reduction is regional-specific in S2-S4 scenarios, a regional-specific efficiency factor $\beta_{r,A\text{-}B}$ is also defined: $(\frac{\Delta X}{X})_B = \beta_{r,A-B} \times (\frac{\Delta E}{E})_A$, where A denotes the region where emissions are reduced, and B denotes the region where the impact is evaluated. For example, $\beta_{r,NC\text{-}SC}$ of sulfate denotes the sensitivity of sulfate concentration change over SC to SO_2 emission reduction over NC. Here the regional $\frac{\Delta E}{E}$ is 0.08 for all the regions in S1, 0.213 for NC in S2, 0.295 for SC in S3, and 0.489 for SWC in S4 scenario. Since the S1 scenario does not have a regional-specific reduction in emissions, the regional sensitivity factor is simply $\beta_{r,B.}$ All the β and $\beta_{r,A\text{-}B}$ are displayed in Figure 6.

3.2 Response of surface SO_2 and sulfate concentrations

In the S1 scenario, a uniform 8% of reduction in SO_2 emissions (totally 2.3Tg)

over China results in a 7.9% and 5.7% decrease of SO_2 and sulfate concentration, respectively, and the corresponding national mean efficiency factor β is 0.99 for SO_2 and 0.71 for sulfate (Figure 6a). Sulfate efficiency factor is smaller than that of SO_2, indicating the nonlinear response of sulfate to SO_2 emission change due to chemistry and transport. The reduction of regional-mean sulfate concentration ranges from 6.2% in SC ($\beta_{r,\,SC}$ = 0.78) to 7.2% in NC ($\beta_{r,\,NC}$ = 0.9). The regional efficiency factors of sulfate over NC, SC and SWC are all greater than the national-mean value, indicating higher emission control efficiency for sulfate by reducing SO_2 emissions from regions with higher emissions. Seasonally, sulfate concentration decrease is smaller in winter than summer at all three regions, indicating that SO_2 emission changes have larger influence on sulfate in summer.

In the S2 scenario, SO_2 emissions from NC are reduced by 21.3%, equivalent to a reduction of 2.3 Tg or 8% of the national total, while emissions from the rest of the country remain unchanged. SO_2 concentration decrease is 19.6% for NC ($\beta_{r,\,NC\text{-}NC}$=0.92), 2.5% for SC ($\beta_{r,\,NC\text{-}SC}$=0.08), and 0.9% for SWC ($\beta_{r,\,NC\text{-}SWC}$=0.04). The annual-mean efficiency factor is 1.0 for national mean surface SO_2. The S2 scenario results in a 14.4%, 4.9% and 3.0% decrease of annual-mean sulfate concentrations over NC, SC, and SWC, respectively. β for national mean sulfate concentration is 0.76, larger than that in S1 (0.71). The regional sulfate efficiency factors (β_r) to SO_2 emission change over NC are: $\beta_{r,\,NC\text{-}NC}$ = 0.68, $\beta_{r,\,NC\text{-}SC}$ = 0.23, and $\beta_{r,\,NC\text{-}SWC}$ = 0.14 (Figure 6b and c). The $\beta_{r,\,NC\text{-}NC}$ of both SO_2 and sulfate in the S2 scenario is smaller than $\beta_{r,\,NC}$ in S1, because the S1 scenario includes reduced transport of SO_2 and sulfate

313 resulting from decreased emissions outside NC. The fact that $\beta_{r,\ NC\text{-}SC}$ and $\beta_{r,\ NC\text{-}SWC}$
314 are both significantly larger than zero indicates the important impact of NC emissions
315 on SO_2 and sulfate concentrations over other regions by way of inter-regional
316 transport. The fact that $\beta_{r,\ NC\text{-}SC}$ is 64% larger than $\beta_{r,\ NC\text{-}SWC}$ provides a clear indication
317 that SO_2 emissions from NC has a larger influence on SO_2 and sulfate concentrations
318 over SC than those over SWC (Figure 6c). The inter-regional efficiency factors ($\beta_{r,}$
319 $_{NC\text{-}SC}$ and $\beta_{r,\ NC\text{-}SWC}$) for sulfate is much larger than those for SO_2 reflecting the longer
320 atmospheric lifetime of sulfate.

321 In the S3 scenario in which SO_2 emissions from SC are reduced by 2.3 Tg or
322 29.5%, the efficiency factor is 0.94 and 0.69 for national mean SO_2 and sulfate
323 concentration, respectively, both smaller than the corresponding values in S1 and S2.
324 For SO_2, there is a 25.1% decrease of SO_2 concentrations over SC and the
325 corresponding $\beta_{r,\ SC\text{-}SC}$ is 0.85. Because of the short lifetime of SO_2 in the atmosphere,
326 the SO_2 inter-regional efficiency factors are much smaller ($\beta_{r,\ SC\text{-}NC}$ = 0.08, and $\beta_{r,}$
327 $_{SC\text{-}SWC}$ = 0.04). Sulfate concentrations decrease by 14.8% over SC, and the
328 corresponding efficiency factor $\beta_{r,\ SC\text{-}SC}$ is 0.50. Compared with $\beta_{r,\ NC\text{-}NC}$ of 0.68 in S2,
329 the lower $\beta_{r,\ SC\text{-}SC}$ in S3 indicates that sulfate over SC is less sensitive to within-region
330 SO_2 emission change than that over NC. The regional efficiency factor of sulfate over
331 NC to changing SC emissions ($\beta_{r,\ SC\text{-}NC}$) is 0.14 for the annual mean, lower than $\beta_{r,}$
332 $_{NC\text{-}SC}$ of 0.23 derived from S2. Seasonally, SO_2 emissions from SC have a larger
333 influence on sulfate over NC in summer ($\beta_{r,\ SC\text{-}NC}$ = 0.16) than winter ($\beta_{r,\ SC\text{-}NC}$ = 0.11),
334 because of different prevailing wind directions in the two seasons. Sulfate

concentrations over SWC have a small sensitivity to changing SO_2 emissions from SC, with a $\beta_{r,\ SC\text{-}SWC}$ of only 0.05.

The S4 scenario, which reduces SO_2 emissions from SWC by 48.9%, has the least effect on national mean sulfur (both SO_2 and sulfate) concentration ($\beta = 0.91$ for SO_2 and 0.68 for sulfate). Sulfate concentrations over SWC have a relatively small efficiency factor to within-region SO_2 emission changes with the $\beta_{r,\ SWC\text{-}SWC}$ of 0.50. $\beta_{r,\ SWC\text{-}NC}$ and $\beta_{r,\ SWC\text{-}SC}$ are both less than 0.05 for sulfate, indicating the limited impact of SO_2 emissions on other regions due to the terrain of Sichuan Basin.

To summarize the above analysis of the four emission scenarios, we find that among the three regions selected, national mean surface concentrations of both SO_2 and sulfate are most sensitive to SO_2 emission changes from NC. SO_2 emissions from NC are 36% and 129% higher than those from SC and SWC, respectively. Because of the short lifetime of SO_2, reducing SO_2 emissions from one region has a small effect on SO_2 concentrations over the other regions, and thus the national-mean SO_2 concentration is most sensitive to SO_2 emissions from NC. Sulfate over NC shows the largest sensitivity to within-region emission changes ($\beta_{r,\ NC\text{-}NC} = 0.68$, compared with $\beta_{r,\ SC\text{-}SC}$ of 0.50 and $\beta_{r,\ SWC\text{-}SWC}$ of 0.50). Sulfate has a longer atmospheric lifetime than SO_2 and can be transported over long distance. SO_2 emission reductions over NC thus have the largest influence on sulfate over adjacent regions with $\beta_{r,\ NC\text{-}SC}$ and $\beta_{r,\ NC\text{-}SWC}$ the largest among the regional efficiency factors of inter-regional transport. As a result, the national-mean β of sulfate is the highest in the S2 scenario (0.76), followed by S1 (0.71), and the mechanism to explain this regional difference will be further discussed

in Section 4. The above analysis indicates that a nationwide uniform reduction of SO_2 emissions may not be the most effective way to reduce surface SO_2 and sulfate concentrations, and SO_2 emission reduction over NC should receive a higher priority in the national policies.

3.3 Response of population-weighted sulfate concentration

Compared with the area-mean sulfate concentration, the population-weighted sulfate concentration (PWC) is a better metric to reflect the public exposure to atmospheric sulfate aerosols because it considers the spatial heterogeneity of population distribution. The PWC is calculated for each province or region by two steps (Stedman et al., 2002): first multiplying the surface sulfate concentration by the population data for individual model grids, then summing up the values of all grids within a province or region and dividing the sum by the total population to get the PWC for each province or region. The population data over China were adopted from SEDAC (SocioEconomic Data and Applications Center, http://sedac.ciesin.columbia.edu/data/collection/gpw-v3) for the year 2010. The original population data from the SEDAC database is at the resolution of about 5 km x 5 km ((1/24)°×(1/24)°). We regridded them to the resolution of 0.5°×0.667° to match with that of the sulfate concentrations from the model.

The annual mean sulfate concentrations and provincial PWC are displayed in Figure 7. Higher sulfate concentrations and PWCs occur over the east and southwest part of China, in accordance with the spatial distribution of anthropogenic SO_2 emissions (c.f. Figure 1). The annual mean sulfate concentration is highest over SWC

(9.9 μg m^{-3}), followed by NC (9.7 μg m^{-3}) and SC (8.1 μg m^{-3}). The annual mean PWC over NC, SC and SWC is 11.2 μg m^{-3}, 9.8 μg m^{-3} and 12.7 μg m^{-3}, respectively. The highest provincial PWC is the Sichuan province (including Chongqing) in SWC and the Hubei province in SC. The correlation between sulfate concentration and population density is stronger over SC and SWC than that over NC. As a result, SWC and SC exert higher weightings in the PWC metric than in the area-mean concentration metric.

The effects of the four emission scenarios on PWC in China are summarized in Table 2. The S3 scenario shows the largest decrease of PWC, with an 8.3% reduction in mean PWC of the three regions and 7.8% for the whole country. The S2 scenario has the second-largest impact, with the corresponding change of 7.6% and 7.5% respectively. The efficiency factor of the national mean PWC is highest in S3 (0.98) and lowest in S1 (0.81). This regional difference indicates that SO_2 emission reductions in SC (i.e., S3) is the most effective way to reduce human exposure to ambient sulfate aerosols, while the national-mean scenario (S1) is the least effective.

3.4 Response of sulfur outflow to the Pacific

Previous studies have found that pollution outflow from East Asia to the Pacific peaks in spring (Chin et al., 2007; Clarisse et al., 2011), while winter is also a significant contributor to the annual outflow flux (Feng et al., 2007). We calculate the sulfur flux to Western Pacific in each scenario for the winter and spring seasons. The transport flux is evaluated at the boundary of 123 °E and 22 °N - 42 °N within the troposphere and the sulfur flux includes both SO_2 and sulfate. We define eastward flux

as positive. The sulfur fluxes for both seasons are positive, indicating net export of sulfur compounds from China to the Western Pacific. Figure 8a displays the seasonal fluxes of each scenario. The standard simulation gives a flux of 490 kt S $month^{-1}$ in winter and 450 kt S $month^{-1}$ in spring. Compared with the standard simulation, the S1 scenario shows a 5.4% decrease of sulfur flux in winter and 5.3% in spring, with the mean value of β being 0.67 for average fluxes of the two seasons. The S2 scenario shows the largest sulfur flux decrease of 7.2% in winter and 8.0% in spring and mean β of 0.95, indicating that SO_2 emission control over NC has the strongest effects on reducing sulfur fluxes to the Western Pacific. The S3 and S4 scenarios have a much smaller impact compared to S1 and S2, and the S3 scenario results in the least response ($\beta = 0.50$). This can be explained by the contribution of each region to the transport fluxes, which will be discussed in Section 4.2.

In summary, the comparison between the different spatial-realizations of the same amount of SO_2 emission reduction for China reveals different impacts not only by region but also by the impact metrics of choice. Reducing SO_2 emissions over NC results in the highest efficiency in reducing surface sulfur concentration in China as a whole with an efficiency factor of 1.0 for SO_2 and 0.76 for sulfate as well as in reducing transport of sulfur to the Western Pacific with the mean β of 0.95. On the other hand, the sensitivity of population-weighted sulfate concentration is highest in the S3 scenario ($\beta = 0.98$), so SO_2 emission control in SC is most effective to reduce human exposure to sulfate aerosols over China.

4. Regional differences in sulfur chemistry and transport

To better understand mechanistically the regional differences in the efficiency factors presented in Section 3, we investigate in this section the regional differences in the conversion of SO_2 to sulfate and inter-regional transport of the major sulfur compounds (SO_2 and sulfate) on the basis of GEOS-Chem model outputs. Sensitivity tests of our findings to meteorology and emissions are also presented.

4.1 SO_2 conversion to sulfate

We have presented in Section 3.2 that the sensitivity of sulfate concentrations to local SO_2 emission changes differs from region to region, and the regional efficiency factor of SO_2 emission control is larger in NC ($\beta_{r,\ NC\text{-}NC}$) than other regions (i.e., $\beta_{r,\ SC\text{-}SC}$ and $\beta_{r,\ SWC\text{-}SWC}$). Here we attribute this difference to regional characteristics of sulfate chemistry using the GEOS-Chem model. As described in Section 2.1, in the model SO_2 is oxidized by OH to form sulfate in the gas phase, or by H_2O_2 and O_3 in the aqueous phase. The two pathways are the main source of atmospheric sulfate. The direct oxidation of SO_2 by O_2 catalyzed by transition metals (Alexander et al., 2009) and the heterogeneous reaction of SO_2 on pre-existing aerosols (Wang Y. et al., 2014) are not included in the current simulation. Globally aqueous phase oxidation plays a larger role than gas phase oxidation in sulfate formation (Unger et al., 2006), while their relative contributions vary regionally and seasonally. In the standard simulation, aqueous phase oxidation of SO_2 contributes 45%, 64% and 73% to sulfate over NC, SC and SWC, respectively. The lower atmospheric humidity and stronger NO_X emissions over NC are two important factors responsible for the higher percentage of gas phase SO_2 oxidation in this region. H_2O_2 oxidation makes up more than 90% of

aqueous phase oxidation for all the three regions. Barth and Church (1999) reported a more than 80% contribution of aqueous phase oxidation to sulfate over Southeast China. Increasing emissions of NO_X and hydrocarbons from China since the 1990s are expected to increase the relative importance of gas phase oxidation for sulfate (Berglen et al., 2004; Unger et al., 2006), which explains the lower fraction of aqueous oxidation in our study.

Table 3 presents the relative changes of SO_2 emissions, SO_2 oxidation rate (gas and aqueous phase and their total), and sulfate concentrations in the regional-specific scenarios (S2-S4) compared with the standard simulation. Reducing SO_2 emissions has different influences on gas and aqueous oxidation. Over all three regions, the relative decrease of gas phase oxidation is greater than that of aqueous oxidation, so the region with a higher contribution from gas phase oxidation will show a larger sensitivity of sulfate to SO_2 emissions reduction; in our study, NC is the region with the largest fraction of gas phase oxidation. Adopting the relationship between the impact metric and SO_2 emission changes defined in Section 3, we derive the regional sensitivity of SO_2 oxidation to be 0.76 for NC (S2), larger than that of 0.67 for SC (S3) and 0.64 for SWC (S4), explaining the larger response of sulfate over NC to within-region SO_2 emissions than the other two regions.

SO_2 emission changes affect both gas- and aqueous-phase oxidation processes, but the magnitude of the influence depends on whether the process is SO_2-limited or not. In most-polluted areas with high NO_X emissions (like China), the aqueous oxidation tends to be oxidants limited rather than SO_2-limited because of the impact

of high-NO_X concentrations on OH, H_2O_2, and O_3. Previous sensitivity studies (Berglen et al., 2004) have found that the gas-phase oxidation is more limited by SO_2. Therefore, SO_2 emission change will have a stronger impact on gas phase oxidation than aqueous phase oxidation and this explains why when SO_2 emissions decrease, the relative decrease of gas phase oxidation is larger than that of aqueous phase oxidation. Since the proportion of gas phase oxidation in NC (55%) is much larger than that in SC (36%) and SWC (27%), the total SO_2 oxidation rates in NC is more sensitive to SO_2 emission changes than those over SC and SWC.

4.2 Sulfur transport

The decrease of sulfate concentrations for each region is less than the extent that can be attributed to within-region SO_2 oxidation and the difference is due to the transport of sulfur between regions. To further separate the impact of within-region vs. inter-regional transport on sulfate concentrations by region, we conducted additional model experiments in which SO_2 emissions from NC, SC and SWC are zeroed off separately. The difference of sulfate concentrations between the standard simulation and each of the zeroing-off model experiments represents the contribution of SO_2 emissions from the corresponding region with zero emissions. The resulting decomposition of monthly mean sulfate concentrations by SO_2 source region is displayed in Figure 9 for NC, SC, and SWC separately.

For the annual average, within-region SO_2 emissions contribute 68% of sulfate concentrations over NC (Figure 9a), followed by 15% from SC emissions. Seasonally, contributions from SC emissions on NC sulfate range from 10% during winter to 17%

during summer. SO_2 emissions from SWC have a small influence (4%) on sulfate over NC, and the remaining 13% of sulfate over NC is from other source regions. For SC (Figure 9b), only 59% of sulfate comes from SO_2 emitted within SC. NC is an important source region for sulfate over SC, contributing 23% annually and ranging from 11% in winter to 30% in summer. Transport from SWC has a very small contribution of only 4%. For SWC, within-region emissions provide 61% of sulfate (Figure 9c), while transport from NC and SC contributes 10% and 8%, respectively, with the remaining 21% from other source regions. The combined contribution of inter-regional transport among the three regions is 19%, 27%, and 18% to sulfate over NC, SC, and SWC, respectively. The shorter lifetime of sulfate over SC and SWC makes it harder to transport over long distances to downwind regions, so among all the inter-regional transport of sulfate examined here, SO_2 emissions from NC exert the largest impacts to sulfate concentrations in other regions, contributing 23% and 10% to sulfate over SC and SWC, respectively. This explains why $\beta_{r,\ NC\text{-}SC}$ and $\beta_{r,\ NC\text{-}SWC}$ derived from the S2 scenario are larger than the regional sensitivity factors of inter-regional transport in other emission scenarios. As a result, for a given amount of SO_2 emission reduction in China, implementing it over NC is found most effective in getting the largest benefit of reducing surface sulfate concentrations over China as a whole.

We further quantify the contribution of each region to the transport fluxes of total sulfur (SO_2 + sulfate) to the Western Pacific for winter, spring and the mean of the two seasons (Figure 8b). NC is the largest contributor and contributes ~40% of total

fluxes for each season. This explains the largest sensitivity factor of the export fluxes to NC emissions in the S2 scenario ($\beta = 0.95$). The contribution from SWC is the second largest, being 17% in spring and 24.1% in winter and a mean of 20.7% for the two seasons. Most of the export fluxes from SWC are found above the boundary layer and as such they have a small effect on surface sulfate concentrations over NC or SC. SC contributes the least (20%) to the export fluxes, resulting in the smallest sensitivity factor of sulfur export flux to the Western Pacific ($\beta = 0.50$) in the S3 scenario.

4.3 Robustness test

The chemistry of SO_2 conversion to sulfate and the transport of sulfur compounds are dependent on both meteorology and emissions. We used a single year's meteorology and emissions (2010) to derive the efficiency factors. To assess the uncertainty of our analysis to the choice of meteorology and the magnitude of emission reductions, sensitivity tests were carried out by changing the year of meteorology to 2009 and by doubling the amount of SO_2 emissions reductions. The national mean sensitivity factor of surface sulfate concentration, population-weighted sulfate concentration and eastward transport fluxes are calculated and compared with that from the S1-S4 emission reduction scenarios.

First, to examine the sensitivity of the model results to the meteorological fields, we conducted a series of one-year test simulations with the 2009 meteorology. In the tests, we used the same emissions as in the standard simulation and the S1-S4 scenarios. With the 2009 meteorology, the national mean SO_2 and sulfate concentration and eastward transport fluxes are also most sensitive to SO_2 emission

reduction from NC (Figure 6a, green short line). The discrepancy in the value of β between simulation with 2009 and 2010 meteorology is within 5%. The efficiency factors for national mean SO_2 and sulfate concentration and sulfur flux are 1.0, 0.78 and 0.94, respectively, compared with the 1.0, 0.76 and 0.95 from the 2010 meteorology. SO_2 emission reduction in SC is most effective in reducing PWC with the national mean β of 0.94 with the 2009 meteorology, compared to the corresponding value of 0.98 from the 2010 meteorology.

Second, the magnitude of SO_2 emissions reduction is doubled in each of the S1-S4 scenarios to check the sensitivity of model results to emissions. These tests are run for one year and with the 2010 meteorology. The efficiency factor for national mean SO_2 and sulfate concentration, PWC and sulfur transport fluxes to the Western Pacific from this test are displayed in Figure 6a with yellow short line. When SO_2 emission reduction is doubled, the national mean SO_2 and sulfate concentration, and the export sulfur fluxes are also most sensitive to SO_2 emission reduction from NC, and β for national mean PWC is the largest when SO_2 emission reduced from SC. However, there is a relatively significant decrease in the value of β, especially for national mean sulfate concentration and PWC (more than 20%). This indicates that SO_2 oxidation rate becomes less sensitive when SO_2 emission reduction is greater.

Furthermore, SO_2 emission control may accompany with changing emissions of NO_X and VOCs because these pollutants have common sources as SO_2. NO_X and VOCs are precursors of tropospheric O_3, and their emissions change can influence the concentrations of H_2O_2, O_3 and OH. While coal combustion is the dominant source of

555 SO_2, it is not the most important source for NO_X or VOCs (transportation being
556 another equally important source for those species). In addition, the technologies used
557 to control SO_2 emissions from coal power plants cannot remove NO_X or VOCs to the
558 same extent as SO_2. To address the impact of changing emissions of co-emitted
559 species on SO_2 chemistry, we conducted a third set of sensitivity tests considering the
560 extreme circumstance in which NO_X and VOCs emissions are also decreased by 8%,
561 equal to the magnitude of SO_2 emission change in the S1 scenario. The results from
562 this sensitivity test are within ±2% of those from S1 for all the metrics we considered.
563 For example, the decrease of national mean SO_2 and sulfate concentrations is 7.80%
564 and 5.76%, respectively; the corresponding value is 7.90% and 5.70% from the S1
565 simulation. This indicates that the change in NO_X and VOCs emissions as a result of
566 SO_2 emission control processes has a negligible impact on SO_2 oxidation and as such
567 it will not affect the conclusion of this study.

568 In summary, we find SO_2 emissions reduction has a larger influence on gas phase
569 oxidation than aqueous phase oxidation. Because sulfate in NC has the largest relative
570 contribution from gas phase oxidation, NC shows the largest sensitivity to
571 within-region SO_2 emission changes. Besides, inter-regional transport contributes 18%
572 ~ 27% of sulfate over the three regions. SO_2 emissions from NC contribute 23% and
573 10% to sulfate over SC and SWC, respectively, which are the largest among all the
574 inter-regional transport of sulfate. This explains why $\beta_{r,\ NC\text{-}SC}$ and $\beta_{r,\ NC\text{-}SWC}$ are the
575 largest among all the efficiency factors to external emission changes (Section 3.2 and
576 Figure 6c). SO_2 emissions from NC contribute the most (~40%) to the sulfur transport

fluxes from China to the Western Pacific, resulting in the largest sensitivity factor (0.95) of the transport flux in the S2 scenario. Contribution from SC is the least (20%) and thus SO_2 emission reduction from SC has the least influence on the transport flux. The robustness tests demonstrate that the ranking of different scenarios are robust with respect to different meteorology year, different magnitude of SO_2 emission reduction, and changing emissions of the co-emitted species (NO_X and VOCs) as SO_2.

5. Conclusion and discussion

We have designed and compared model sensitivities in which the same amount of SO_2 emission reduction (2.3 Tg, 8% of total SO_2 emission from China in 2010, following the 12^{th} FYP) is implemented uniformly in China as a whole (S1) and in three sub-regions only (NC, SC and SWC) to investigate the emission control efficiencies in different regions. The GEOS-Chem chemical transport model is used in this study to quantify the response of different concentration and flux metrics to SO_2 emissions change.

National mean and inter-regional efficiency factors (β and β_r) are defined as the percentage change of the concerned metrics caused by a 1% decrease of SO_2 emission changes. The metrics include surface SO_2 and sulfate concentrations, the population-weighted sulfate concentration and sulfur transport from China to the Western Pacific. SO_2 emission reduction from NC (S2 scenario) has the largest influence on national mean SO_2 concentration with the efficiency factor of 1.0. The S2 scenario is also most effective in reducing the mean sulfate concentration over

China as a whole with the highest national-mean β of 0.76, which can be explained in two aspects. On one hand, SO_2 oxidation in gas phase is found to be more sensitive to the change of SO_2 emissions than aqueous phase oxidation, and NC is the region with the largest fraction of gas phase SO_2 oxidation. This makes sulfate over NC most sensitive to within-region emission changes with the largest efficiency factor ($\beta_{r,\ NC\text{-}NC}$ = 0.68, $\beta_{r,\ SC\text{-}SC}$ =0.5, $\beta_{r,\ SWC\text{-}SWC}$ = 0.50). On the other hand, comparison of inter-regional sulfate transport reveals that SO_2 emissions from NC exert the largest impacts to sulfate concentrations in other regions (23% for SC and 10% for SWC). This leads to $\beta_{r,\ NC\text{-}SC}$ and $\beta_{r,\ NC\text{-}SWC}$ being the largest among the regional efficiency factors of inter-regional transport.

Among the three regions, NC contributes most (~40%) to the transport fluxes of sulfur from China to the Western Pacific, so the Western Pacific region will benefit most from SO_2 reduction in NC with the mean β of 0.95. Contribution from SC is the least among the three regions studied here, resulting in the smallest efficiency factor of sulfur export flux to the Western Pacific (β = 0.50) in the S3 scenario. We also find that SO_2 emission control in SC is most effective to reduce human exposure to sulfate aerosols over China as a whole, as indicated by the highest sensitivity of population-weighted sulfate concentration in the S3 scenario (β = 0.98). The efficiency factors and their spatial differences are found to be robust and not dependent on the year of meteorology, the magnitude of SO_2 emissions change or the change in emissions of co-emitted NO_X and VOCs.

Based on the analysis above, we recommend that a nationwide uniform reduction

620 of SO_2 emissions may not result in the largest emission control efficiency.
621 Considering that NC makes the largest contribution to inter-regional transport of
622 sulfur within China and to the transport fluxes to the Western Pacific, SO_2 emission
623 reduction over NC should receive a higher priority in the national policies in order to
624 maximize the air quality benefits for China and downwind regions. However, from
625 2006 to 2010 (the 11^{th} Five-Year Plan period), SO_2 emissions from NC have
626 decreased at a much slower rate than the national total emissions. Based on the MEIC
627 inventory, total SO_2 emissions from China were 9.4% lower in 2010 than 2006, and
628 emissions from NC, SC and SWC have decreased by 4.7%, 16.1% and 23.1%,
629 respectively, during the same period. The relative reduction of SO_2 emissions in NC is
630 thus one third or less of that for the other two regions and is only half of the reduction
631 at the national mean level. This indicates that China has not prioritized SO_2 emission
632 control in NC in the past. Our study suggests this should be corrected in the future in
633 order to maximize the benefits of SO_2 control.
634
635 **Acknowledgement**: This research was supported by the National Key Basic Research
636 Program of China (2014CB441302), the CAS Strategic Priority Research Program
637 (Grant No. XDA05100403), and the Beijing Nova Program (Z121109002512052). We
638 thank the free use of surface measurements from EANET, AOD data from MODIS
639 and SO_2 columns data from OMI.
640

References:

Alexander, B., Park, R. J., Jacob, D. J., and Gong, S.: Transition metal-catalyzed oxidation of atmospheric sulfur: Global implications for the sulfur budget, J. Geophys. Res., 114, D02309, doi:10.1029/2008JD010486, 2009.

Barth, M. C., and Church, A. T.: Regional and global distributions and lifetimes of sulfate aerosols from Mexico City and southeast China, J. Geophys. Res., 104(23), 30231-30239, 1999.

Benkovitz, C. M., Scholtz, M. T., Pacyna, J., Tarras ́on, L., Dignon, J., Voldner, E. C., Spiro, P. A., Logan, J. A., and Graedel, T. E.: Global gridded inventories of anthropogenic emissions of sulfur and nitrogen, J. Geophys. Res., 101, 29239–29253, doi:10.1029/96JD00126, 1996.

Berglen, T. F., Berntsen, T. K., Isaksen, I. S. A., and Sundet J. K.: A global model of the coupled sulfur/oxidant chemistry in the troposphere: The sulfur cycle, J. Geophys. Res., 109, D19310, doi:10.1029/2003JD003948, 2004.

Chen, D., Wang, Y., McElroy, M. B., He, K., Yantosca, R. M., and Le Sager, P.: Regional CO pollution and export in China simulation by the high-resolution nested-grid GEOS-Chem model, Atmos. Chem. Phys., 9, 3825–3839, doi:10.5194/acp-9-3825-2009, 2009.

Chin, Mian, Diehl, T., Ginoux, P., and Malm, W.: Intercontinental transport of pollution and dust aerosols: implications for regional air quality, Atmos. Chem. Phys., 7, 5501-5517, doi:10.5194/acp-7-5501-2007, 2007.

Clarisse, L., Fromm, M., Ngadi, Y., Emmons, L., Clerbaux, C., Hurtmans, D., and Coheur, P.-F.: Intercontinental transport of anthropogenic sulfur dioxide and other pollutants: An infrared remote sensing case study. Gephys. Res. Lett., 38, L19806, doi:10.1029/2011GL048976, 2011.

Fairlie, T. D., Jacob, D. J., Dibb, J. E., Alexander, B., Avery, M. A., van Donkelaar, A., and Zhang, L.: Impact of nimeral dust on nitrate, sulfate, and ozone in transpacific Asian pollution plumes, Atmos. Chem. Phys., 10, 3999-4012, doi:10.5194/acp-10-3999-2010, 2010.

Feng , J., Guo, Z., Chan, C. K., and Fang, M.: Properties of organic matter in $PM_{2.5}$ at Changdao Island, China – a rural site in the transport path of the Asian Continental outflow. Atmos. Environ., 41: 1924-1935, 2007.

Fountoukis, C., and Nenes, A.: ISORROPIA II: a computationally efficient thermodynamic equilibrium model for K^+-Ca^{2+}-Mg^{2+}-NH_4^+-Na^+-SO_4^{2-}-NO_3^--Cl^--H_2O aerosols. Atmos. Chem. Phys., 7, 4639–4659, doi:10.5194/acp-7-4639-2007, 2007.

Heald., C. L., Jacob, D. J., Park, R. J., Alexander, B., Fairlie, T. D., Yantosca, R. M., and Chu, D. A.: Transpacific transport of Asian anthropogenic aerosols and its impact on surface air quality in the United Stades, J. Geophys. Res., 111, D14310, doi: 10.1029/2005JD006847, 2006.

He, H., Li, C., Loughner, C. P., Li, Z., Krotkov, N. A., Yang, K., Wang, L., Zheng, Y., Bao, X., Zhao, G., and Dickerson, R. R.: SO_2 over central China: Measurements, numerical simulations and the tropospheric sulfur budget, J. Geophys. Res., 117, D00K37, doi:10.1029/2011JD016473, 2012.

He, K. B.: Multi-resolution Emission Inventory for China (MEIC): model framework and 1990–2010 anthropogenic emissions, International Global Atmospheric Chemistry Conference, 17–21, September, Beijing, China, 2012.

Itahashi, S., Uno, I., Yumlmoto, K., Irie, H., Osada, K., Fukushima, H., Wang, Z., and Phara, T.: Interannual variation in the fine-mode MODIS aerosol optical depth and its relationship to the changes in sulfur dioxide emissions in China between 2000 and 2010, Atmos. Chem. Phys., 12, 2631 – 2640, doi:10.5194/acp-12-2631-2012, 2012a.

Itahashi, S., Uno, I., Kim, S.: Source contributions of sulfate aerosols over East Asia estimated by CMAQ-DDM, Environ. Sci. Technol., 46, 6733-6741, 2012b.

Lamsal, L. N., Martin, R. V., Padmanabhan, A., van Donkelaar, A., Zhang, Q., Sioris, C. E., Chance, K., Kurosu, T. P., and Newchurch, M. J.: Application of satellite observations for timely updates to global anthropogenic NOX emission inventories, Geophys. Res. Lett., 38, L05810, doi: 10.1029/2010GL046476, 2011.

Li, C., Krotkov, N. A., Dickerson, R. R., Li, Z, Yang, K., and Chin, M.: Transport and evolution of a pollution plume from northern China: A satellite-based case study, J. Geophys. Res., 115, D00K03, doi:10.1029/2009JD012245, 2010a.

Lou, S., Liao, H., and Zhu, B.: Impacts of aerosols on surface-layer ozone concentrations in China through heterogeneous reactions and changes in photolysis rates, Atmos. Environ., 85, 123-138, 2014.

Lu, Z., Zhang, Q., and Streets, D. G.: Sulfur dioxide and primary carbonaceous aerosol emissions in China and India, 1996-2010, Atmos. Chem. Phys., 11, 9839 – 9864, doi:10.5194/acp-11-9839-2011, 2011.

Manktelow, P. T., Mann, G. W., Carslaw, K. S., Spracklen, D. V., and Chipperfield, M. P.: Regional and global trends in sulfate aerosol since the 1980s, Geophys. Res. Lett., 34, L14803, doi:10.1029/2006GL028668, 2007.

Park, R. J., Jacob, D. J., Field, B. D., Yantosca, R.M., and Chin, M.: Natural transboundary pollution influences on sulfate-nitrate-ammonium aerosols in the United States: Implications for policy, J. Geophys, Res., 109, D15204, doi:10.1029/2003JD004473, 2004.

Roelofs, G-J., Lelieveld, J., and Ganzeveld, L.: Simulation of global sulfate distribution and the influence on effective cloud drop radii with a coupled photochemistry-sulfur cycle model, Tellus, 50B, 224-242, 1998.

Schreifels, J. J., Fu, Y., and Wilson, J. E.: Sulfur dioxide control in China: policy evolution during the 10th and 11th Five-Year Plans and lessons for the future. Energy Policy, 48(2012) 779-789, 2012.

Stedman, J. R., Grice, S., Kent, A., and Cooke, S.: GIS-based models for ambient PM exposure and health impact assessment for the UK, J. Phys. Conf. Ser., 151(1): 012002, doi:10.1088/1742-6596/151/1/012002, 2002.

Tao, J., Gao, J., Zhang, L., Zhang, R., Che, H., Zhang, Z., Lin, Z., Jing, J., Cao, J., and Hsu, S.-C.: PM2.5 pollution in a megacity of southwest China: source apportionment and implication, Atmos. Chem. Phys., 14, 8679-8699, doi:10.5194/acp-14-8679-2014, 2014.

Unger, N., Shindell, D. T., Koch, D. M., and Streets, D. G.: Cross influences of ozone

and sulfate precursor emissions changes on air quality and climate, PNAS, vol. 103, no. 12, 4377-4380, 2006.

Wang, J., Xu, X., Henze, D. K., Zeng, J., Ji, Q., Tsay, S-C., and Huang, J.: Top-down estimate of dust emissions through integration of MODIS and MISR aerosol retrievals with the GEOS-Chem adjoint model, Geophys. Res. Lett., 39, L08802, doi:10.1029/2012GL051136, 2012.

Wang, L. T., Wei, Z., Yang, J., Zhang, Y., Zhang, F. F., Su, J., Meng, C. C., and Zhang, Q.: The 2013 severe haze over the southern Hebei, China: model evaluation, source apportionment, and policy implications, Atmos. Chem. Phys., 14, 3151-3173, doi:10.5194/acp-14-3151-2014, 2014.

Wang, Y., McElroy, M. B., Jacob, D. J., and Yantosca, R. M.: A nested grid formulation for chemical transport over Asia: Applications to CO, J. Geophys. Res., 109, D22307, doi:10.1029/2004JD005237, 2004.

Wang, Y., Zhang, Q. Q., He, K., Zhang, Q., and Chai, L.: Sulfate-nitrate-ammonium aerosols over China: response to 2000-2015 emission changes of sulfur dioxide, nitrogen oxide, and ammonia, Atmos. Chem. Phys., 13, 2635 – 2652, doi:10.5194/acp-13-2635-2013, 2013a.

Wang, Y., Zhang, Q. Q., Jiang, J., Zhou, W., Wang, B., He, K., Duan, F., Zhang, Q., Philip, S., and Xie, Y.: Enhanced sulfate formation during China's severe winter haze episode in January 2013 missing from current models, J. Geophys. Res., 119, 10425-10440, doi:10.1002/2013JD021426, 2014.

Zhang, F., Cheng, H. R., Wang, Z.-W., Lv, X.-P., Zhu, Z., Zhang, G., and Wang, X.: Fine particles ($PM_{2.5}$) at a CAWNET background site in Central China: Chemical composition, seasonal variations and regional pollution events. Atmos. Environ. 86, 193-202, doi:10.1016/j.atmosenv.2013.12.008, 2014.

Zhang, H., Wu, S., Huang, Y., and Wang, Y.: Effects of stratospheric ozone recovery on photochemistry and ozone air quality in the troposphere. Atmos. Chem. Phys, 14, 4079-4086, doi:10.5194/acp-14-4079-2014, 2014.

Zhang, L., Jacob, D. J., Knipping, E. M., Kumar, N., Munger, J. W., Carouge, C. C., van Donkelaar, A., Wang, Y. X., and Chen, D.: Nitrogen deposition to the United States: distribution, sources, and processes, Atmos. Chem. Phys., 12, 4539-4554, doi: 10.5194/acp-12-4539-2012, 2012.

Zhang, X. Y., Wang, Y. Q., Niu, T., Zhang, X. C., Gong, S. L., Zhang, Y. M., and Sun, J. Y.: Atmospheric aerosol compositions in China: spatial/temporal variability, chemical signature, regional haze distribution and comparisons with global aerosols, Atmos. Chem. Phys., 12, 779 – 799, doi:10.5194/acp-12-779-2012, 2012.

Tables

Table 1: simulation scenarios and SO_2 emission in each study

Simulation scenario	description	SO_2 emission (Tg)			
		China	NC	SC	SWC
standard	Standard, 2010 inventory	28.4	10.8	7.8	4.7
S1	SO_2 emission is reduced uniformly across China by 8% (2.3 Tg)	26.1	9.9	7.2	4.3
S2	Implement 2.3 Tg SO_2 reduction on NC, emission from other regions unchanged	26.1	8.5	7.8	4.7
S3	Implement 2.3 TgSO_2 reduction on SC, emission from other regions unchanged	26.1	10.8	5.5	4.7
S4	Implement 2.3 TgSO_2 reduction on SWC, emission from other regions unchanged	26.1	10.8	7.8	2.4

Table 2: change in population-weighted sulfate concentrations, μg m^{-3}

		Difference with the standard simulation			
	standard simulation	S1	S2	S3	S4
NC+SC+SWC	10.9	-6.7%	-7.6%	-8.3%	-7.1%
China	9.7	-6.6%	-7.5%	-7.8%	-6.9%

Table 3: percentage changes of SO_2 conversion to sulfate and sulfate concentration over NC, SC and SWC in response to within-region SO_2 emission changes:

	SO_2 emission	SO_2 conversion			Sulfate concentration
		Gas phase	Aqueous phase	total	
NC (S2)	-21.3%	-20.6%	-10.4%	-16.1%	-14.4%
SC (S3)	-29.5%	-22.6%	-17.1%	-19.9%	-14.8%
SWC (S4)	-48.9%	-41.8%	-30.1%	-31.4%	-24.5%

782 **Figures**

783

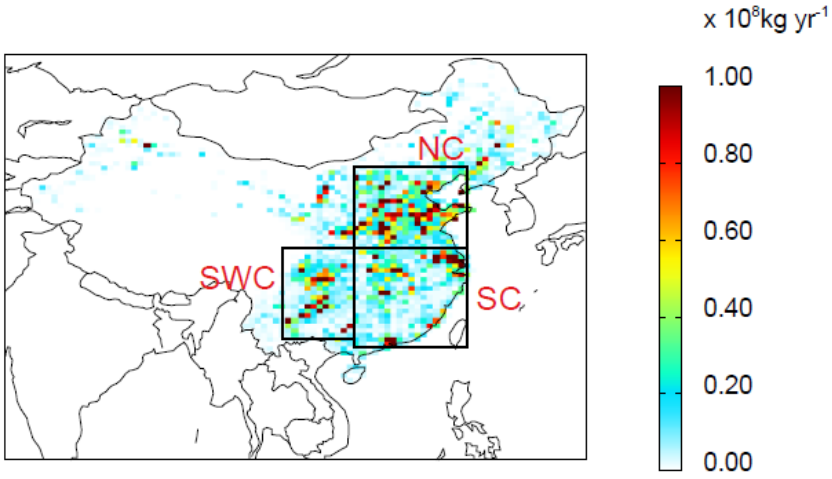

784

785 **Figure 1. SO_2 emissions from China in the year of 2010.**

786

787

788

789

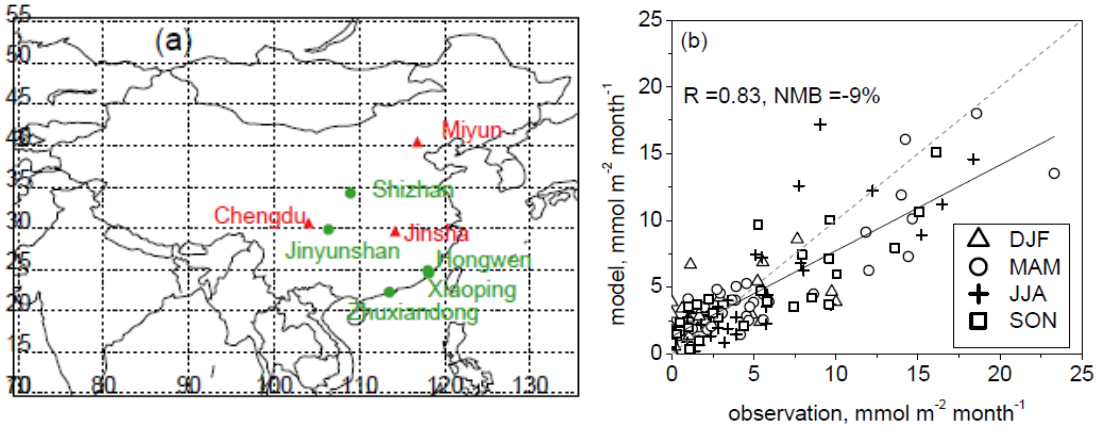

790

791 **Figure 2. (a) Locations of observation sites. The red triangles represent sites with surface**
792 **sulfate concentration, and the green dots represent sites with sulfate wet deposition fluxes. (b)**
793 **Scatter plot of simulated versus observed sulfate wet deposition fluxes in 5 sites over China,**
794 **from January 2009 to December 2010.**

795

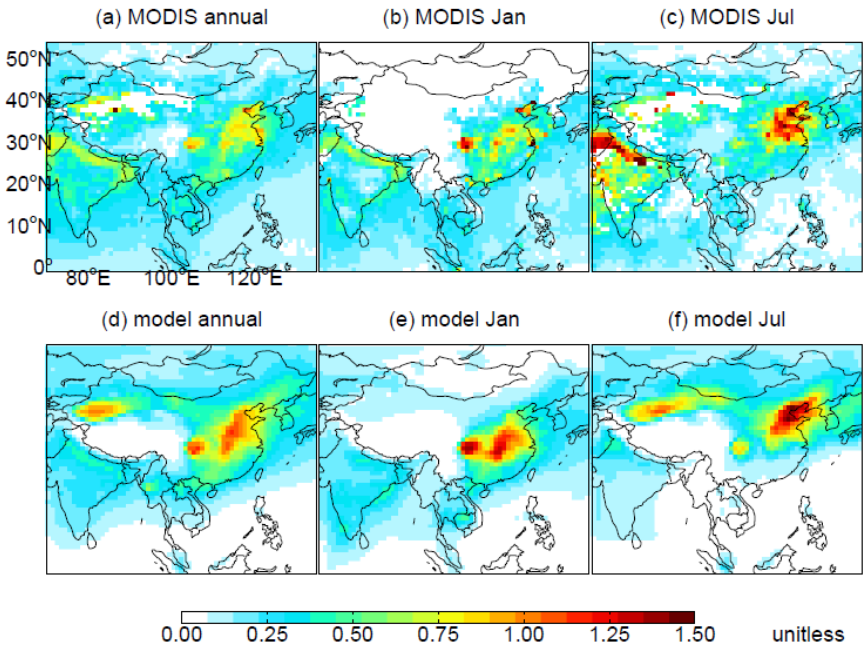

796

797 **Figure 3. Aerosol optical depth (AOD) over East Asia from MODIS for (a) 2010 annual mean,**

798 **(b) January, and (c) July, and from the GEOS-Chem model: (d) annual mean, (e) January,**

799 **and (f) July.**

800

801

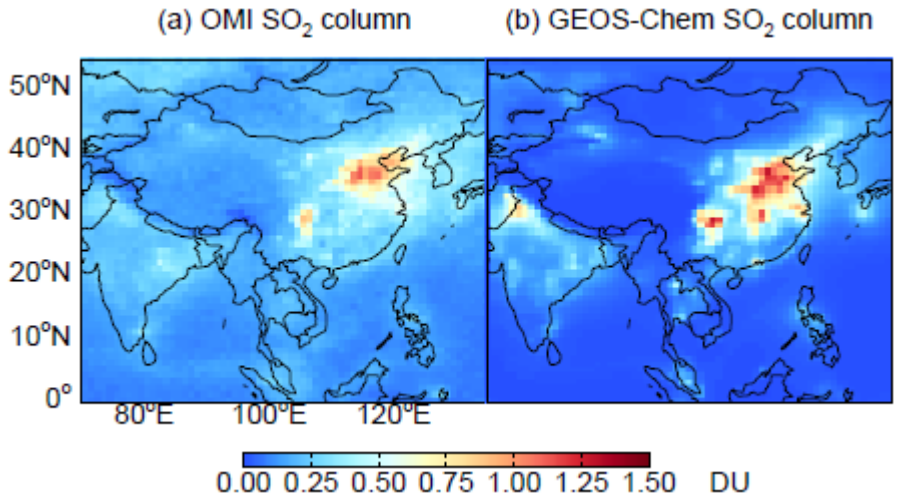

802

803 **Figure 4. Annual mean total SO_2 columns from (a) OMI satellite instrument and (b)**

804 **GEOS-Chem simulation for the year 2010.**

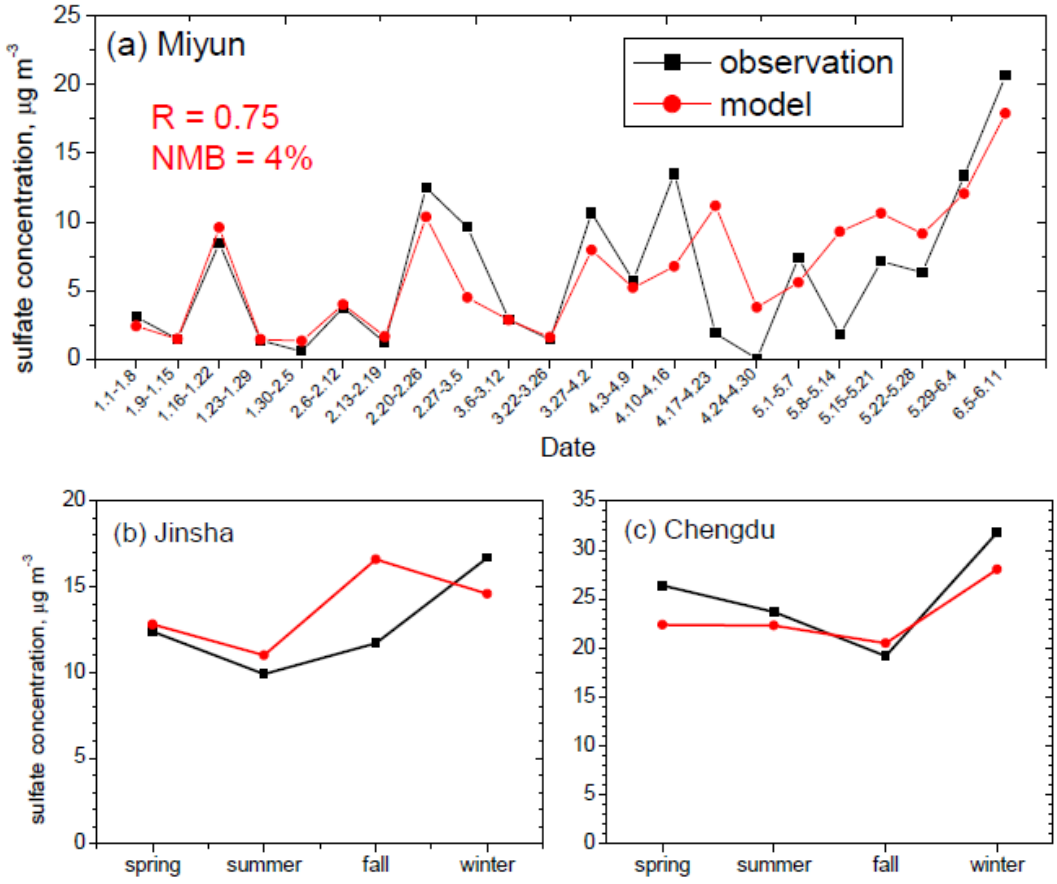

Figure 5. Comparison of observed (black line) and simulated (red line) surface sulfate concentrations at (a) Miyun site with weekly sulfate concentration from January to June in 2010; (b) Jinsha site with seasonal mean sulfate concentration from Zhang et al. (2014), and the observation year is 2012; (c) Chengdu site with monthly mean sulfate concentration from Tao et al. (2014), the observation time is January, April, July, and October in 2011.

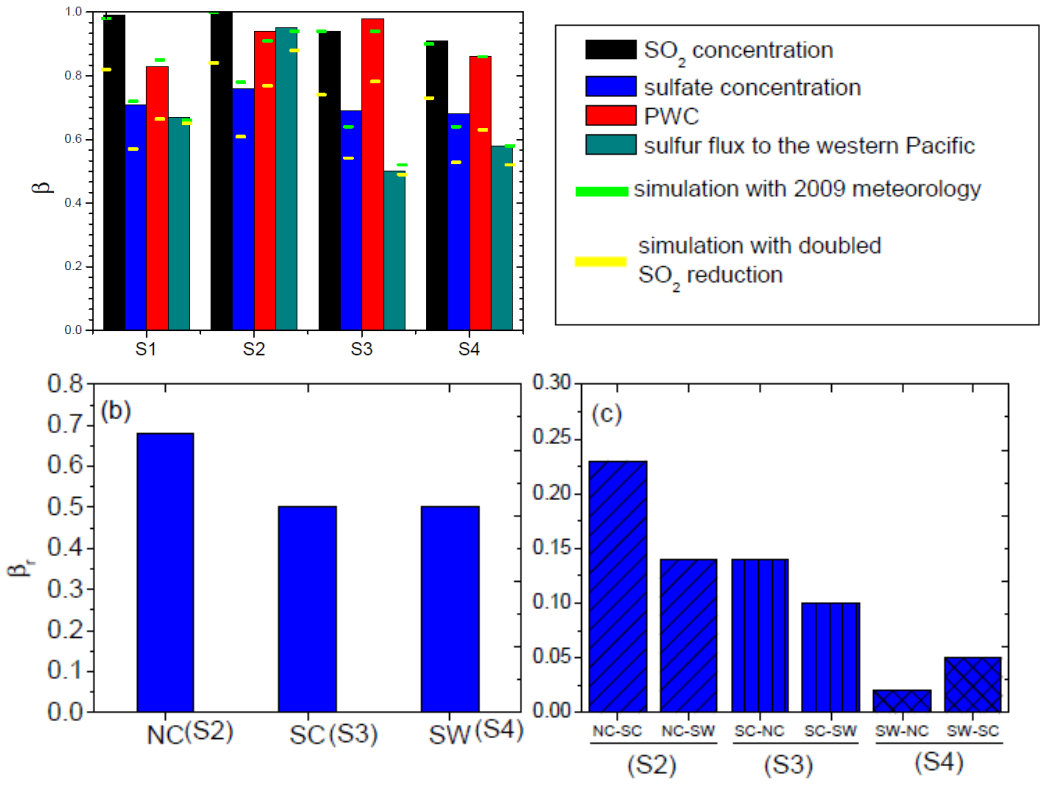

818

819 **Figure 6. (a) Emission control efficiency factors (β) of national mean SO_2 and sulfate**
820 **concentrations, population-weighted sulfate concentrations (PWC), and sulfur fluxes from**
821 **China to the west Pacific in S1-S4 simulation scenarios. (b) Regional efficiency factors (β_r) of**
822 **sulfate concentrations over NC, SC and SWC to within-region SO_2 emission changes. (c)**
823 **Inter-regional efficiency factor by scenario. The efficiency factor of national mean sulfate**
824 **concentrations, PWC, and eastward sulfur transport fluxes in the robustness sensitivity tests**
825 **are presented in (a): the green short line represents results from simulation with meteorology**
826 **for 2009, the yellow short line represents results from doubled magnitude of SO_2 emission**
827 **reduction simulation.**

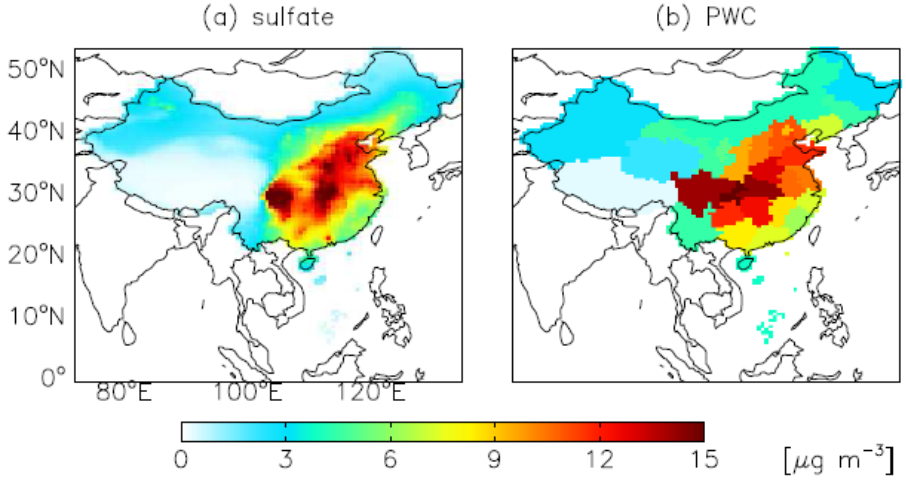

828 **Figure 7. Annual mean sulfate concentration and population-weighted sulfate concentration**

829 **over China (sulfate and population data of Taiwan Province are not available).**

830

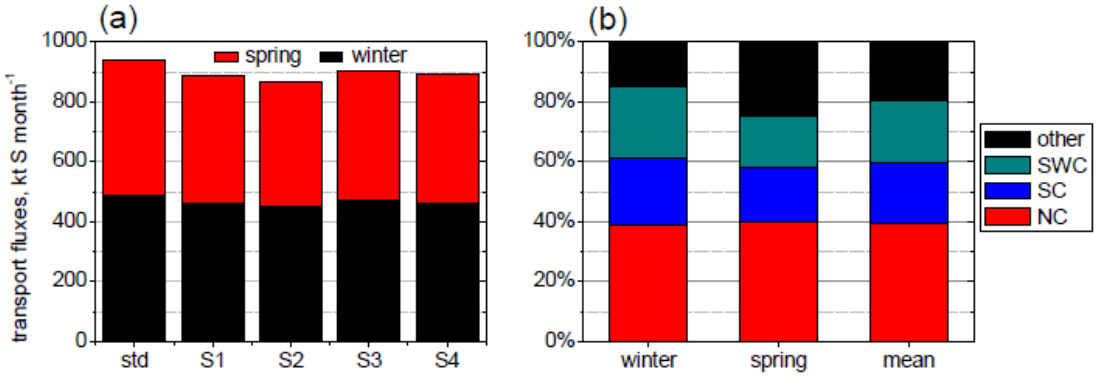

831

832 **Figure 8. (a) Sulfur (SO_2 + sulfate) flux at the 123 °E, 22 °-42 °N tropospheric plane from**

833 **China to the Western Pacific, and (b) percentage contribution of NC, SC, SWC and other**

834 **regions (the rest of Chinese regions as well as global influence) to sulfur (SO_2 + sulfate)**

835 **transport fluxes from China to the Western Pacific.**

836

837

838

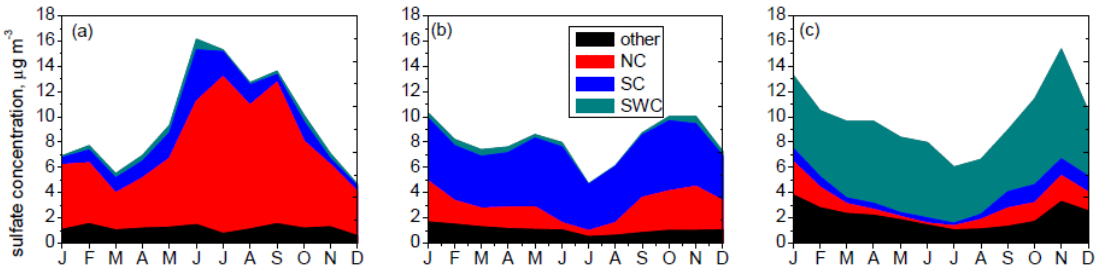

Figure 9. Monthly and regional mean sulfate concentrations over (a) NC, (b) SC and (c) SWC, with contributions from within-region and inter-regional transport. Here "other" includes the rest of Chinese regions as well as foreign influence.